AIAA-2000-4888

CONSTRUCTING VARIABLE FIDELITY RESPONSE SURFACE APPROXIMATIONS IN THE USABLE FEASIBLE REGION

Victor M. Pérez * **John E. Renaud** † **Shawn E. Gano** ‡

Department of Aerospace and Mechanical Engineering
University of Notre Dame
Notre Dame, Indiana
Email: John.E.Renaud.2@nd.edu

Abstract

The use of Response Surface Approximation (RSA) within an approximate optimization framework for the design of complex systems has increased as designers are challenged to develop better designs in reduced times. Traditionally, statistical sampling techniques (i. e., experimental design) have been used for constructing RSA's. These statistical sampling techniques are designed to be space £lling, so that the response surface approximations are predictive across the range of the design sample space. When used in sequential approximate optimization strategies, a portion of the samples can be in the infeasible and/or ascent regions of the design space. These samples can bias the resulting RSA and make it less predictive in the usable feasible region where the optimization takes place. In the response surface based concurrent subsace optimization approach the design sampling strategy for RSA construction is optimization based. This optimization based sampling has proved to be effective due to the fact it samples in the linearized usable feasible region. In the present research, an experimental design strategy for projecting data points in the linearized usable feasible region is developed for constructing RSA's. The technique is implemented in a Sequential Approximate Optimization framework and tested in application to two multidisciplinary design optimization (MDO) test problems. Results show that the proposed technique produces a more accurate RSA in the usable feasible region as compared to using conventional statistical sampling.

Nomenclature

$\mathbf{a}_i$	Projection Vector
$\mathbf{A}$	Householder Matrix
$\mathbf{d}$	Directional Vector
$\mathbf{D}$	DOE Array
$\mathbf{E}$	Matrix of Sampling Points.
f	Merit Function
$\mathbf{g}$	Constraints vector
$\mathbf{I}$	Identity Matrix
$\mathbf{T}$	Transformation Matrix
$\mathbf{x}_0$	Current Design Point
$\nabla\mathbf{f}$	Function Gradient
$\nabla\mathbf{g}_i$	Constraint Gradient

1 Introduction.

The increased availability of high speed, lower cost computing has powered the development of high £delity computational models by designers in most engineering disciplines. However the high cost of computation associated with invoking these models prevents them from being used in optimization, where reaching a solution may requires hundreds or even thousands of analysis calls. Because of this, there has been a growing interest

*Graduate Research Assistant, Student Member AIAA.
†Associate Professor, Associate Fellow AIAA.
‡Undergraduate Research Assistant.

in the use of lower £delity Response Surface Approximations (RSA) as surrogate models within an optimization framework for Multidisciplinary Design Optimization (MDO).

The RSA strategies for optimization can be divided into two broad categories. Strategies that attempt to build RSA's that span the entire design space[7,9−11,16,17,26,28,35] and strategies that sequentially build response surface approximations within a local trust region[1−4,18,20−25,32,36−39]. Our research focuses on the latter approach, where the notion of the usable feasible region can be evaluated at each sequential iterate using the gradient information of the objective and constraints.

In a Sequential Approximate Optimization (SAO) algorithm, at each new iteration, a RSA of the objective function and each constraint is constructed after executing the analysis tools at each experimental design site about the current design point. The RSA's are used as surrogates of the objective function and constraints. Approximate optimization subject to move limits results in an a new design point. There are three basic features in SAO which differentiate one algorithm from another. First, the sampling technique used to build the RSA around the current design point. Second, the move limit strategy, which de£nes where to sample and how far to go in the optimization, and £nally the driving algorithm that de£nes not only the merit function, but the overall control of the parameters in the program. This investigation focuses on the sampling technique used to generate the RSA's.

There exist basically two different approaches for sampling in a SAO framework. The £rst one is a traditional statistically based sampling using Design of Experiments (DOE) techniques. The objective function and constraints are evaluated at the design points from the experimental array. The resulting database is then used to build a RSA. A variety of statistically based sampling strategies such as central composite design (CCD)[23], orthogonal arrays (OA)[19,15], D-optimality criteria[13] and DACE[7] are all very effective in generating response surface approximations.

The other approach, is an optimization based sampling, which has roots in the original Concurrent SubSpace Optimization (CSSO) algorithm of Sobieski [29], later modi£ed for response surface approximate optimization in Renaud and Gabriel[20, 21] and re£ned in Wujek *et al.*[37], and Rodriguez *et al.*[23]. Each of the subdisciplines perform an optimization subject to move limits. Linear approximations to the required input states are used. The design sites visited through the subspace optimizations are stored and serve as the database for the RSA construction. The design sampling strategy is optimization based and therefore the design samples tend toward feasibility and descent. However, the CSSO strategy is not statistical in nature and generates ribbons of data in each subspace.

In a recent study by Rodríguez *et al.* [24], OA's were introduced to build RSA's within a MDO framework. The OA's generate a rich sampling within the TR. Results show that while strength 2 orthogonal arrays seem to perform well compared to the CSSO approach of Rodríguez *et al.* [23], CSSO is still more robust in driving the optimization. Strength 2 OA's have a big advantage over traditional DOE techniques. The number of design points for an OA with n design variables is order n^2 while a traditional DOE array as a 2 levels full factorial (FF) or CCD are order 2^n. Note that the number of terms required for approximating a 2*nd* order polynomial RSA is order n^2.

One of the big differences between the two approaches is based on the fact, that CSSO samples mostly in the approximate usable-feasible region; moreover, this is not a linearized region but a curved path due to the sequential nature of the approach. Figure 1 shows a statistical sampling array around a current design point. The linearized usable-feasible region is bounded by the lines orthogonal to the function and the constraint gradient. Note that the region we are most interested in is being sampled with only a portion of the sample points in a traditional DOE array.

In this research a new approach for design space sampling is being investigated. We propose to project experimental arrays from DOE techniques such as OA's into the usable feasible region[40] for design space sampling. The resulting design samples will be both space-£lling and will have properties of feasibility and descent. The £rst part of the paper describes the methodology to create this type of sampling. In the second part of the paper an implementation of the projected sampling methodology is incorporated in the Trust Region Augmented Lagrangian algorithm presented by Rodríguez *et al.*[23] is tested. The effectiveness of the resulting RSA's are studied using two example MDO problems.

2 Methodology

A matrix of experiments can be visualized as an hypercube populated by design points. Such a hypercube can be de£ned by orthogonal vectors that form the basis of the design space. Each of these vectors corresponds

to a design variable. In Rodríguez *et al.*[24] the matrix of experiments was scaled and translated to surround the current point with sample points bounded by the trust region as shown in Figure 1. This approach is referred to as conventional sampling in this study. In this work we locate the current design point in a corner of the matrix of experiments and rotate the hypercube to point it towards the usable feasible region. This section describes the methodology developed in this research to generate samples in the linearized usable feasible region.

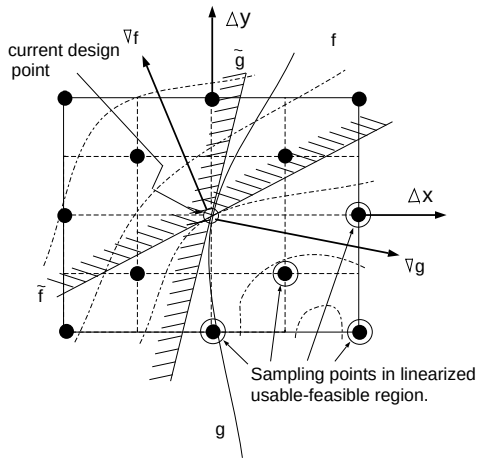

Figure 1. OA sampling in a 2D design space

In a 2D design space, the linearized usable feasible region is de£ned by two vectors that happen to be either normal to the gradient of the function or to any of the gradients of the active constraints. A de£nition of the basis can be easily formulated and we can populate design points within the limits of the linearized usable feasible region as is shown in Fig. 2. From this £gure we can see that a problem may arise. The basis that de£nes the usable-feasible region is not orthogonal in almost all the cases. As a result, the array is squeezed into a space much smaller that the original sampling region. This problem will be revisited later when we state the formulation for £nding the basis.

For the case of a design space in $\mathbb{R}^n$ with $n > 2$, the usable feasible region can not be de£ned by a basis of n vectors because the linearized region is de£ned by hyperplanes orthogonal to the function gradient or to the gradients of the constraints. It is impossible to £nd a set of vectors that will de£ne entirely the usable feasible region as in the 2D space. However we can still de£ne a set of vectors that capture the majority of the linearized usable-feasible region.

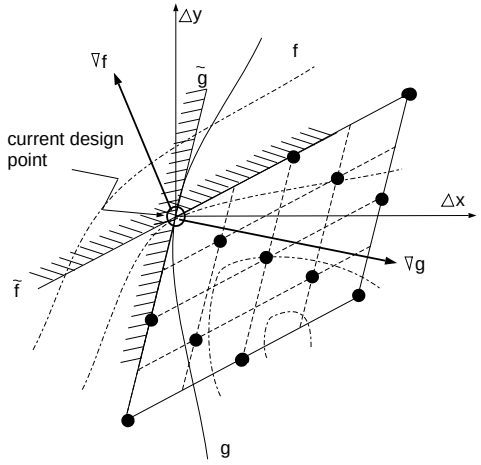

Figure 2. Projected OA sampling in a 2D design space

Formulations

The problem is to £nd a set of unit vectors $\mathbf{a}_i$ that satisfy two conditions. The £rst one is that they can be used to de£ne a space primarily in the usable feasible region. The second condition is that the vectors must be as close as orthogonal as possible. The £rst condition relates to the main idea of this research, the latter to the desire to avoid squeezing the array, creating a sampling array in a slender region.

For the following formulations, we assume the standard form of a non-linear constrained optimization problem with inequality constraints of the form $g \geq 0$. Equality constraints do not enter in any formulation but can be present in the problems.

2.1 Formulation I

A simple formulation for £nding the basis is:

$$\min_{w.r.t.\mathbf{a},\alpha} \quad \alpha \tag{1}$$

$$\text{s.t.} \quad \mathbf{a}_i^T \mathbf{a}_j \leq \alpha \qquad i,j = 1..n, i \neq j \tag{2}$$

$$\mathbf{a}_i^T \mathbf{a}_j \geq -\alpha \qquad i,j = 1..n, i \neq j \tag{3}$$

$$\mathbf{a}_i^T \nabla f \leq 0 \qquad i = 1..n \tag{4}$$

$$\mathbf{a}_i^T \nabla \mathbf{g}_j \geq 0 \qquad i = 1..n, j = 1..m \tag{5}$$

$$\mathbf{a}_i^T \mathbf{a}_i = 1 \qquad \text{i=1 .. n} \tag{6}$$

This formulation provides a set of normal vectors which are strictly in the linearized usable-feasible region. At the same time the minimization pushes the vectors to be as close to orthogonal as possible.

2.2 Formulation II

In a variation of the £rst formulation we force the vectors to be orthogonal, but some of them might be out of the linearized usable-feasible region:

$$\min_{w.r.t.\,\mathbf{a},\alpha} \quad \alpha \tag{7}$$

$$\text{s.t.} \quad \mathbf{a}_i^T \mathbf{a}_j = 0 \qquad i,j = 1..n, i \neq j \tag{8}$$

$$\mathbf{a}_i^T \nabla \mathbf{f} \leq \alpha \qquad i = 1..n \tag{9}$$

$$-\mathbf{a}_i^T \nabla \mathbf{g}_j \leq \alpha \qquad i = 1..n, j = 1..m \tag{10}$$

$$\mathbf{a}_i^T \mathbf{a}_i = 1 \qquad \text{i=1 .. n} \tag{11}$$

Both Formulation I and II introduce a minimization subproblem required within each iteration of the SAO algorithm. Moreover, the dimension of the subproblems is n^2+1 and there is no unique solution. This subproblem might become expensive and it has to be repeated at each iteration. Therefore there is a need for a simpler formulation that avoids such complex minimization problems.

2.3 Formulation III

The third formulation differs from the previous two in that there is no need for a minimization subproblem. Assume we can £nd a vector **d** which points to the usable-feasible region. We can generate an orthogonal basis $\mathbf{a_i}$ around the vector **d** that projects toward the linearized usable-feasible region. Note that the vectors that form the basis might point to the infeasible region, however most of the space bounded by such vectors will be located in the feasible region. Each of the infeasible vectors can be projected onto the most violated constraint hyper-plane, generating a strictly feasible non-orthogonal basis. In the following paragraphs we discuss in detail each of the steps required in such projection.

2.3.1 Sampling direction. Many of the methods of optimization for NLP use the concept of a search direction and a line search to reduce the value of the merit function. Depending of the algorithm used to drive the optimization, one can choose between constrained and unconstrained line search directions. If the merit function is a penalty function or an Augmented Lagrangian, one can use an unconstrained search direction (steepest descent, conjugate gradient, quasi-Newton), however if we are interested in a strict descent feasible direction, we can use Zoutendijk's usable-feasible direction[40] or the direction obtained solving the quadratic subproblem in the SQP approach. In this research one makes use of conventional search directions as a basis for de£ning a sampling direction.

In Rodríguez *et al.*[24] and in this research the Augmented Lagrangian is used as the merit function. Therefore the natural sampling direction to be used is the descent direction, however because the variable bounds are not included when constructing the Augmented Lagrangian, the concept of projected gradient will be used[22].

2.3.2 Construction of the orthogonal basis. Once the sampling (i. e. search) direction has been found, the next step is to construct an orthogonal basis around this search direction. This is done in a very ef£cient manner with the help of the Householder transformation [12].

Let's de£ne a unit vector **s** with components $\mathbf{s}_i = \frac{1}{\sqrt{n}}$, where n is the number of design variables. This unit vector is surrounded by n unit vectors $\mathbf{e}_i$ that form an orthogonal basis that correspond to each of the axis of the design space. The angle between **S** and each $\mathbf{e}_i$ is given by $\cos\theta = \mathbf{s}^T \mathbf{e}_i = \frac{1}{\sqrt{n}}$. Assuming that our search direction **d** is a unit vector. There exists an orthonormal linear transformation $\mathbf{A} = \mathbf{A}^T$ formed by unit vectors $\mathbf{a}_i$ such that $\mathbf{A}\,\mathbf{s} = \mathbf{d}$ and the unit vectors $\mathbf{a}_i$ form the orthogonal basis around **d** that we are looking for, as $\mathbf{A}\mathbf{e}_i = \mathbf{a}_i$ and $\mathbf{a}_i^T \mathbf{d} = \frac{1}{\sqrt{n}}$.

The orthonormal matrix **A** can be generated by use of the Householder transformation.[12]

A Householder transformation matrix **A** is de£ned by a vector **u** as:

$$\mathbf{A} = \mathbf{I} - \frac{1}{2}\mathbf{u}\mathbf{u}^T, \tag{12}$$

where **u** is the vector that joins **d** and **s** scaled by a magnitude $\frac{1}{C}$. To simplify we make $\mathbf{r} = \mathbf{d} - \mathbf{s}$ and so

$$\mathbf{u} = \frac{\mathbf{r}}{C}, \tag{13}$$

substituting (13) into (12) we obtain:

$$\mathbf{A} = \mathbf{I} - \frac{1}{2}\frac{\mathbf{r}\mathbf{r}^T}{C^2}, \tag{14}$$

where C has to be chosen such that:

$$\mathbf{A}\,\mathbf{s} = \mathbf{d}. \tag{15}$$

Substituting (14) into (15) we obtain:

$$-\frac{1}{2C^2}\mathbf{r}\mathbf{r}^T\mathbf{s} = \mathbf{d} - \mathbf{s}. \tag{16}$$

Note that $\mathbf{r}^T\mathbf{s}$ is a scalar and $\mathbf{d} - \mathbf{s} = \mathbf{r}$. Therefore:

$$-\frac{1}{2C^2}\mathbf{r}^T\mathbf{s} = 1, \tag{17}$$

so we can £nd C as:

$$C^2 = -\frac{1}{2}\mathbf{r}^T\mathbf{s}, \tag{18}$$

$$C^2 = \frac{1}{2}(1 - \mathbf{d}^T\mathbf{s}). \tag{19}$$

Finally substituting (19) into (14) gives:

$$\mathbf{A} = \mathbf{I} - \frac{\mathbf{r}\mathbf{r}^T}{1 - \mathbf{d}^T\mathbf{s}}. \tag{20}$$

Note that the unit vectors $\mathbf{a}_i$ could lay on the infeasible region, but most of the sampling would be oriented towards the usable-feasible region.

2.3.3 Projection of the basis to the feasible region. Once the orthogonal basis is computed, we can check for feasibility of each of the unit vectors. Given the gradients of the active constraints at the current design point $\nabla\mathbf{g}_j$ we look for pairs $\{i, j\}$ such that $\nabla\mathbf{g}_j^T\mathbf{a}_i < 0$. A new feasible unit vector $\tilde{\mathbf{a}}_i = \alpha\mathbf{a}_i + \beta\nabla\mathbf{g}_i$ can be computed such that $\nabla\mathbf{g}_j^T\tilde{\mathbf{a}}_i = 0$ and $\|\tilde{\mathbf{a}}_i\|_2 = 1$, which replaces those vectors $\mathbf{a}_i$ that point to the infeasible region. These approach is referred as the projected non-orthogonal array in this research.

There are two basic disadvantages of building a set of non-orthogonal projection vectors. The £rst one is that it might generate a very slender polytope loosing the richness of the £lling sought with OA. The second one relates to the fact that the linearized usable feasible region might not coincide with the actual non-linear usable feasible region.

2.3.4 Scaling of the basis. Once the basis is set, it has to be scaled to meet the current trust region. For this process it is important that all the design variables have proper scaling. The search direction vector **d** is extended until it reaches the TR bound. Then it is projected onto the basis. Each of the projected components form the transformation matrix**T**. The new transformation matrix **T** is formed by a set of non unit vectors that de£ne a polytope pointing toward the descent direction which are scaled to the size of the TR.

2.3.5 Computation of design points. Finally to de£ne the array of design points **E** to be sampled by the algorithm, we £rst, project the matrix of experiments **D** onto the basis **T**, and second, translate it to the current design point.

These two operations can be done as follows:

$$\mathbf{E} = \frac{1}{nl}\mathbf{T}\cdot\mathbf{D}^T + \mathbf{x}_0 \tag{21}$$

3 Test Problems

To test the new method, two MDO problems tested in the Rodríguez *et al.*[24] study of OA's are used. The driving algorithm for the optimization is the Trust Region Augmented Lagrangian introduced by Rodríguez *et al.*[22,24]. The algorithm is based in an Augmented Lagrangian merit function. The sampling direction **d** is de£ned as the negative of the projected gradient of the Augmented Lagrangian.

3.1 The Control-Augmented Structure

The structures-controls design problem shown in Figure 3 was introduced by Sobieski *et al.*[31]. The problem includes a total of 11 design variables and 43 states. The physical problem consists of a cantilever beam subjected to static loads along the beam and to a dynamic excitation force applied at the free end. Two sets of actuators are placed at the free end of the beam to control both the lateral and rotational displacement.

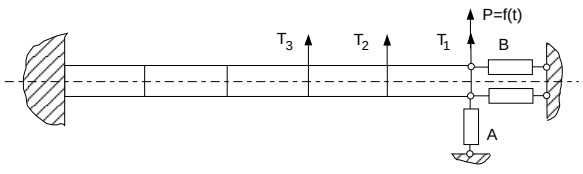

Figure 3. Control-Augmented Structure.

The system analysis is comprised of two coupled contributing analysis as shown in Figure 4. The structures subsystem, CA_s consists of a £nite element model of the beam where the natural frequencies and modes of the cantilever beam are computed. CA_s requires, in addition to the characteristics of the beam, the weight of the control system as input. The weight of the control system is calculated at the controls CA, CA_c. The weight of the control system is a function of the dynamic displacements and rotations of the free end of the beam. These dynamic displacements and rotations are functions of the natural frequencies and modes obtained in the structures CA, thus subjecting these CAs to coupling.

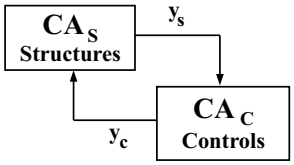

Figure 4. Dependency diagram of the CAS design problem.

The objective of the optimization is to minimize the total weight of the system W_t, composed of the weight of the beam W_s plus the weight of the control system W_c. The minimization is subjected to seven constraints on the static stresses (σ), static lateral and rotational displacements (dl and dr), the £rst two natural frequencies (ω_1 and ω_1) and dynamic lateral and rotational displacements at the free end of the beam (ddl and ddr). The problem is posed as:

$$\min W_t = W_s + W_c$$

subject to

$$g_1 = 1 - \frac{dl}{dl_a} \geq 0,$$
$$g_2 = 1 - \frac{dr}{dr_a} \geq 0,$$
$$g_3 = \frac{\omega_1}{\omega_{1_a}} - 1 \geq 0,$$
$$g_4 = \frac{\omega_2}{\omega_{2_a}} - 1 \geq 0,$$
$$g_5 = 1 - \frac{\sigma}{\sigma_a} \geq 0,$$
$$g_6 = 1 - \frac{ddl}{ddl_a} \geq 0,$$
$$g_7 = 1 - \frac{ddr}{ddr_a} \geq 0,$$

3.2 Autonomous Hovercraft

The design of an autonomous hovercraft (AHC), shown in Figure 5, was £rst presented in Sellar *et al.*[27]. This problem involves 11 design variables and the calculation of 50 states. The physical system consists of an engine, rotor, and payload. The rotor is comprised of two rectangular lifting surfaces located on opposite ends of a hollow, circular shaft. The system is to operate such that the motor speed (RPM) provides a thrust-to-weight ratio of one, imposing a hover condition.

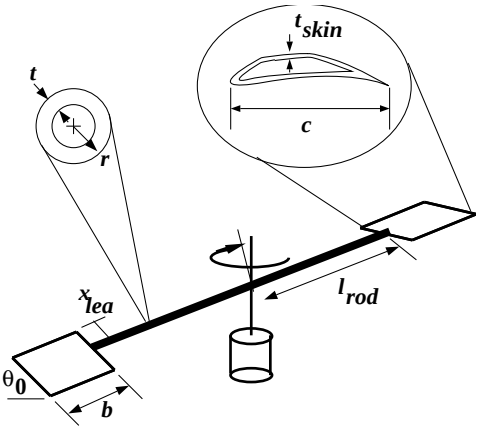

Figure 5. Autonomous hovercraft system.

The system analysis is comprised of four contributing analysis, three of which interact in a complex coupled fashion as illustrated in the dependency diagram of Figure 6. The aerodynamics CA (CA_a) calculates the aerodynamic loads on the lifting surfaces and approximates the distributed drag force along the rod while estimating the induced velocity at the lifting surfaces as a function of the thrust. CA_a requires the torsional deformation of the shaft (θ_d), the motor RPM and thrust as inputs. The shaft deformation is supplied by the structures CA (CA_s). All the quantities calculated by this CA, which also include the axial and shear stresses at the hub and the de¤ection of the lifting surfaces, are a function of the aerodynamic loads, thus subjecting these CA's to static aeroelastic coupling. The propulsion/performance CA (CA_p) calculates the thrust and torque necessary to spin the motor based on the loads supplied by CA_a. RPM is calculated by explicitly imposing that the total weight equals the thrust, determining the weight of the motor to achieve this total weight, and calculating the power and resulting RPM available from that size motor. The fourth CA, structural dynamics (CA_d), calculates the £rst natural frequencies of the rotor in bending and torsion. This CA is completely uncoupled from the other CA's as it requires no states as inputs.

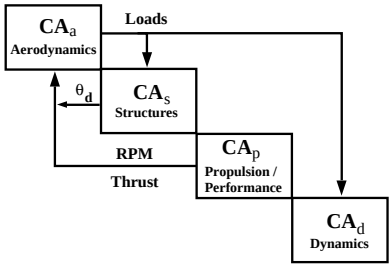

Figure 6. AHS dependency diagram.

The goal of the optimization of this system is to minimize the empty weight of the hovercraft subject to constraints on the Von Misses stress due to in-plane (σ_N) and normal forces (σ_T) in the rod, the £rst natural frequencies of the rod (ω_b and ω_t), the Mach number at the tip ($M_{tip_{all}}$), and the hovercraft range (E). The global optimum for this problem was £rst reported in Sellar.[?]. The optimization problem is posed as:

$$\min W_{empty} = W_{wing} + W_{rod} + W_{fuel} + W_{motor}$$

subject to

$$g_1 = 1.0 - \frac{\sigma_N}{\sigma_{all}} \geq 0.0,$$
$$g_2 = 1.0 - \frac{\sigma_T}{\sigma_{all}} \geq 0.0,$$
$$g_3 = \frac{\omega_b}{k \cdot RPM} - 1.0 \geq 0.0,$$
$$g_4 = \frac{\omega_t}{k \cdot RPM} - 1.0 \geq 0.0,$$
$$g_5 = \frac{M_{tip_{all}}}{M_{tip}} \geq 0.0,$$
$$g_6 = \frac{E}{E_{req}} - 1.0 \geq 0.0.$$

4 Testing Methodology

To test the projected sampling methodology developed in this paper, we use the trust region managed augmented Lagrangian algorithm introduced by Rodríguez *et al.*[22] The variable £delity analysis approach implemented in Rodríguez *et al.*[24] is used for analysis at the projected sampling sites. One of the advantages of the Rodríguez algorithm is that the trust region management strategy insures convergence through proper management of the move limits in the sequential minimization. The augmented Lagrangian approach translates the nonlinear constrained minimization problem into an unconstrained minimization problem with variable bounds. In this case, the sampling direction **d** is de£ne as the descent direction of the augmented Lagrangian, taking into account the variable bounds by means of the projected gradient. The projected gradient is computed within the algorithm for the convergence check and therefore their is no additional cost imposed when using the new projected sampling strategy.

The sampling strategy is similar to that used in Rodríguez *et al.* [24] The experimental array is a strength 2 OA with 8 levels for 11 design variables. The OA is randomized after each iteration with respect to the 11 design variables. Using the projected methodology developed in this research, at each iteration the basis is computed and the OA projected into it. The design points generated by the projected array are sampled in each of the decoupled contributing analysis. This strategy was reported as the most successful one among a suite of strategies compared in Rodríguez *et al.* [24] A second order RSA of the objective and each constraint are built using the queried data.

A comparison between the projected array proposed in this paper and the conventional statistical sampling used in Rodríguez *et al.*.[24] is performed for both test problems. The third technique compared is the projected non orthogonal sampling, i. e. with the basis strictly feasible as described in subsection 2.3.3.

5 Results

5.1 Control Augmented Structure

5.1.1 Computational cost. In the following table we compare the cost as the total number of approximate minimizations. The optimization was performed ten times for each case. The same initial design point was used for the ten repetitions, however a different initialization for the random generator was required at each run. The results represent the mean and standard deviation of the number of iterations..

	Conventional	Projected	Projected n/o
Mean	40	37	67
Variance	11	11	16

Table 1. Mean value of the total number of approximate minimizations for the CAS problem

Introduction of the projected sampling strategy does not signi£cantly improve the mean while the variance remains without change. The projected non orthogonal sampling requires an increased number of approximate minimizations with a larger standard deviation. One possible explanation why the projected sampling strategy does not perform signi£cantly better than the conventional centered orthogonal array might be related to the nature of the sampling direction as we approach the optimum. In the trust region managed augmented Lagrangian approach, a successive minimization of the augmented Lagrangian is performed as part of an inner loop with a £xed set of multipliers. Once convergence in the inner loop is reached, the multipliers are updated and another sequence of minimizations is performed. The projected gradient of the augmented Lagrangian becomes very small as the algorithm approaches convergence. As the projected gradient approaches zero, the sampling direction becomes dif£cult to compute accurately due to round off errors in the analysis tools. The sampling methodology proposed is based on the use of the projected gradient as the sampling direction. If the projected gradient is inaccurate, the sampling direction is inaccurate too, and the sampling is performed in a direction different than the desired one. A second explanation might be that the traditional centered OA sampling produces RSA's that approximate the augmented Lagrangian accurately and therefore the projected sampling strategy does not perform better.

The projected non-orthogonal sampling has a very poor performance. The augmented Lagrangian algorithm used for minimization is basically an external point method. One or several constraints are violated throughout the optimization. If several constraints are violated or active at a given point the linearized feasible region might be too narrow. The projected non-orthogonal array of experiments is squeezed into that region and a very poor experimental design is obtained.

5.1.2 TR/SR ratio γ. Another way to visualize if the projected array provides a better approximation to the function is through the use of the trust region test.[2,3,38,39]

The trust region approach is based on the use of a trust region ratio ρ to monitor how well the current approximation is found to represent the actual design space. Considering an *unconstrained* problem with an objective function Φ which is approximated by a function $\tilde{\Phi}$, the trust region ratio is de£ned as

$$\rho^{(t)} = \frac{\Phi(\mathbf{x}^{(t)}) - \Phi(\mathbf{x}^{(t+1)})}{\Phi(\mathbf{x}^{(t)}) - \tilde{\Phi}(\mathbf{x}^{(t+1)})} \tag{22}$$

This is simply the ratio of the actual change in the function to the change predicted by the approximation. The closer the value of ρ to one, the better the approximation $\tilde{\Phi}$ mimics the behavior in the descent direction of Φ. After each optimization iteration (t), the trust region radius is updated according to the following principles:

1. If the ratio is negative or small, the iteration is considered unsuccessful since either the actual objective increased (it is known that $\tilde{\Phi}$ will not increase) or it did decrease, but not nearly as much as predicted by the approximation. In either case, the approximation is certainly poor and the trust region must be reduced.
2. Conversely, if the ratio is close to one, a reasonable decrease in the objective function has been observed relative to the approximate decrease, and the iteration is considered successful. It should be noted that if the ratio is signi£cantly larger than one, the objective function actually decreased more than had been predicted, and the approximation is actually a poor representation of the design space. However, since this scenario is actually favorable as more reduction is gained than expected, it is considered as a successful iteration.
3. Finally, if the ratio is an intermediate value, the wisest choice of action may be to leave the size of the trust region as it is.

Mathematically, the above rules for updating the trust region radius may be described by choosing constants to de£ne the ranges of the ratio value for which reduction or enlargement are necessary. The positive constants $R_1 < R_2 < 1$ and $c_1 < 1, c_2 > 1$ are chosen so that the trust region radius Δ (% change allowed for each design variable) is updated as

$$\Delta^{(t+1)} = \begin{cases} c_1\Delta^{(t)} & \text{if } \rho^{(t)} < R_1 \\ c_2\Delta^{(t)} & \text{if } \rho^{(t)} > R_2 \\ \Delta^{(t)} & \text{otherwise} \end{cases} \tag{23}$$

Typical values for the limiting range values are $R_1 = .25$ and $R_2 = .75$. The trust region multiplication factors c_1 and c_2 have been chosen in to be .25 and 2 respectively.

In this research, we de£ne a new term referred to as the Sampling Region (SR). In the current implementation the sampling region is the same as the trust region for the current iterate. The projected OA used in this research is therefore bound by the current trust region. Testing indicates that the RSA's developed using the projected OA

sampling are predictive beyond the trust region bounds. Therefore in future studies we plan to independently assign the trust region and sampling region.

To illustrate the more predictive RSA's generated using the projected OA sampling, we can change the size of the TR used for optimization, and perform a trust region test to see how predictive the approximation is beyond the sample region. We control how far beyond the current SR we extend the TR by the introduction of a TR/SR ratio γ. For each value of γ we perform a minimization of the RSA. A trust region test is performed and the value of the trust region ratio ρ is queried. Figures 7, 8 and 9 show the results for three different points in the optimization. The £gures show results for the projected, the projected non-orthogonal and the conventional cases.

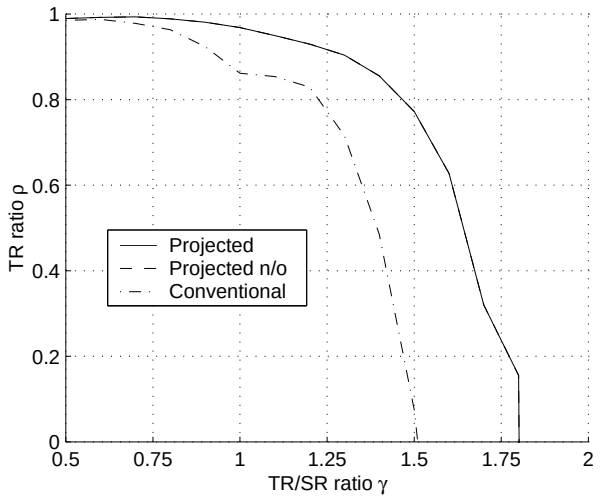

Figure 7. Trust Region ratio ρ vs. TR/SR ratio γ for the CAS problem

Figure 7 corresponds to an initial feasible point. When the ratio γ approaches zero, the TR ratio goes to one because the RSA is a second order Taylor series expansion. When $\gamma = 1$ the values of the TR ratios differ but not enough to alter the control of the TR (see Equation 23 in the augmented Lagrangian process. However as the TR/SR γ increases, the RSA from the projected sampling provides a much better approximation. At $\gamma = 1.5$ the TR ratio for the projected sampling is still very good $\rho = 0.8$ whereas the conventional OA leads to $\rho = 0.0$. Eventually both curves end up having negative values but we could make more progress in the optimization using the projected sampling strategy. Because no constraint is violated, the curve for the projected and projected non-orthogonal cases are the same.

Figure 8 shows a different design point. We clearly

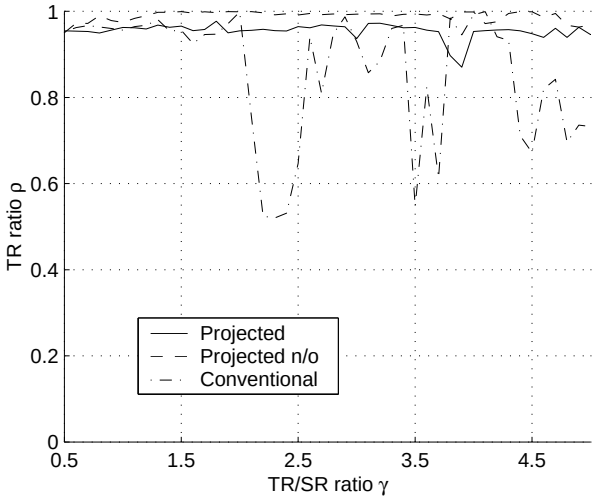

Figure 8. Trust Region ratio ρ vs. TR/SR ratio γ

see that the projected and the projected non-orthogonal samplings generate a very good RSA as the value of the TR ratio is nearly 1 even for big values of the γ ratio. For the given SR, the RSA predicts the behavior of the function very well, at least in the descent direction. The conventional sampling also does a good job for moderate values of γ, however at large values of the ratio, ρ is very unstable in its response, although ρ maintains a value above 0.5. For this design point, the RSA for the projected non-orthogonal sampling exhibits slightly better performance than the orthogonal projection.

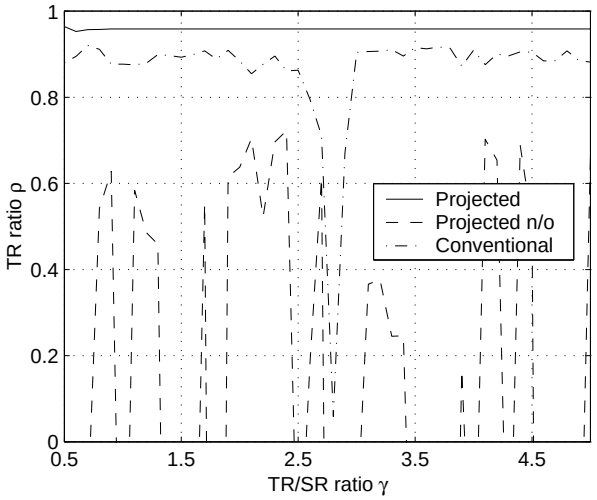

Figure 9. Trust Region ratio ρ vs. TR/SR ratio γa

When several constraints are active or violated and tend to oppose each other with respect to feasibility,

an interesting effect is noticed as shown in Figure 9. The projected sampling generates a good approximation, however the projected non-orthogonal results in a very unstable approximation that switches between positive and negative values in a sudden manner. The response for the conventional sampling is good, except for a small interval where it deteriorates.

5.2 Autonomous Hovercraft

5.2.1 Computational cost. For the AHS problem, the results are very interesting. In all three cases, the mean value of the number of approximate minimizations remains the same while the value of the standard deviation increases for the case of the projected sampling and for the projected non-orthogonal sampling. Table 2 summarizes the results.

	Conventional	Projected	Projected n/o
Mean	15	15	15
Variance	3	7	4

Table 2. Mean value of the total number of approximate minimizations for the AHS problem.

5.2.2 TR/SR ratio Three different design points were evaluated. Their corresponding behaviors are shown in Figures 10-12 for the the AHS. The projected, projected non-orthogonal and conventional samplings are displayed. In Figure 10 the projected sampling exhibits better performance in the approximation of the function. Close to $\gamma = 1$ the value of the TR ratio is very similar for the three approaches, however the difference between projected and conventional increases as γ is increased. The projected non-orthogonal approach has a response that oscillates between the projected and the conventional approach. Note that the rate of decrease in the TR ratio ρ reduces as γ is increased.

In Figure 11 the three approaches exhibit similar behavior. There is no noticeable difference for the range of γ explored. It might be that the function is very close to a quadratic about the current design point and no matter how the sampling is performed, a good approximation is obtained. With $\gamma > 2$ the curve becomes ¤at. When γ is small, the result of the minimization over the RSA lays on the bounds of the TR. As γ is increased the minimum (both of the true function and of the RSA) keeps moving

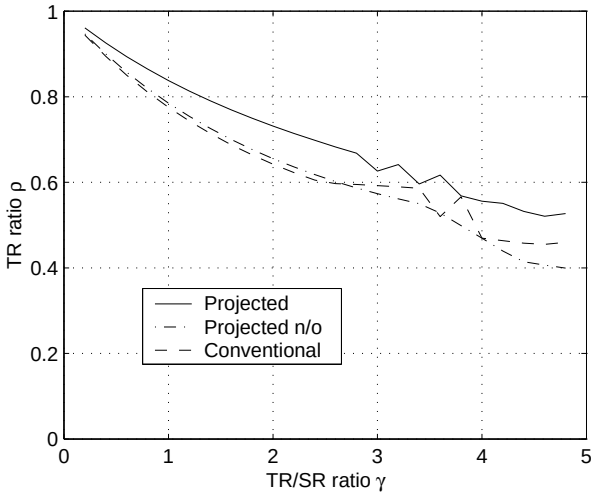

Figure 10. Trust Region ratio ρ vs. TR/SR ratio γ

with the bounds until it is within the bounds. After that even if the bounds are enlarged, the value of the minimum won't change. Another reason for the curve to ¤atten out is when the bounds of the TR reach the variable bounds of the problem in the direction of the minimization.

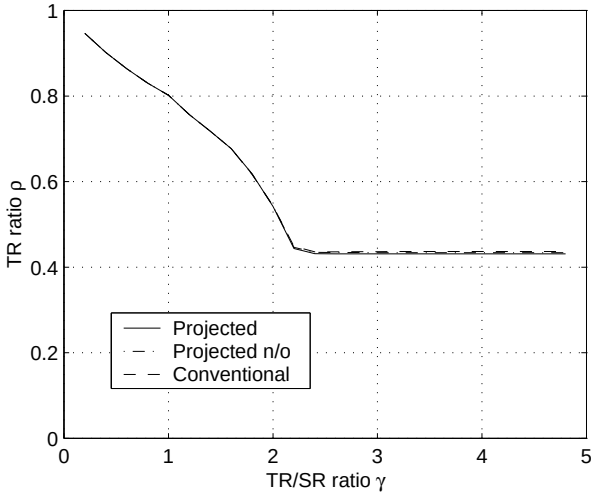

Figure 11. Trust Region ratio ρ vs. TR/SR ratio γ

Finally in Figure 12 the projected and projected non-orthogonal samplings have almost the same performance, with a slight advantage observed for the latter. The response for the conventional sampling is just below them, with a bigger difference for small values of γ. As in Figure 10 the slope decreases as γ is increased.

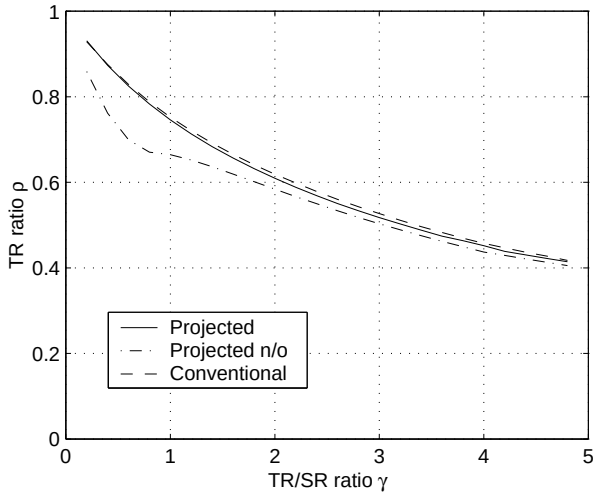

Figure 12. Trust Region ratio ρ vs. TR/SR ratio γ

6 Discussion

The projected sampling described in this paper is capable of providing a RSA suitable for optimization. The projected sampling queries more points in the descent feasible direction, generating a richer database for construction of the RSA. The improvement in RSA performance when using projected sampling, does not affect directly the overall performance of the optimization, measured by the total number of approximate minimizations. This can be explained with the help of Figures 7, 9 and 10. Note that when $\gamma = 1$ the value of the TR ratio for both the projected and the conventional sampling are similar in value. Because of this the trust region used in the next iteration will be the same for both methods (see Equation 23). Therefore even though the projected OA generates an improved RSA, no appreciable difference is observed in optimization convergence rate. In future research, the development of a dynamic control strategy for setting the TR independently from the SR will be investigated. We hope to exploit the improved RSA to speed convergence.

When we force the projection to be strictly in the approximate feasible region (i. e. projected non-orthogonal), we obtain non-desirable effects. The hypercube de£ned by the orthogonal basis is squeezed into a slender polytope. The sampling volume is reduced, while the corner completely opposite to the current design point is pushed away. As a result the sampling is relatively rich along the line between those two points, but poor around the polytope. More importantly, the sampling may not capture the behavior of the constraints in the infeasible region, when they are active, which is the case at the constrained optimum. This phenomena is observed in Table 1 where both the number of approximate minimizations and the standard deviation are increased with the use of the non-orthogonal projection. On the other hand this effect is not noticeable for the AHS as shown in Table 2. The difference in behavior between the two problems re¤ects the instability of the projected non-orthogonal sampling, when several constraints are active or violated. Figures 8 and 9 show this negative effect.

7 Conclusions

A technique to project an orthogonal array into the linearized usable-feasible region to construct response surface approximations (RSA) for sequential approximate optimization is presented. The technique has been implemented successfully within a trust region managed augmented Lagrangian approach. Two multidisciplinary design optimization (MDO) test problems are used to evaluate the utility of the projected array for RSA construction. Results show that the RSA's obtained using the projected sampling strategy are more predictive in the usable feasible region when approximating the response of the augmented Lagrangian function. Although the new RSA's are more predictive, no appreciable difference in the number of approximate minimizations required to converge the optimization was observed. The current trust region model management strategy does not exploit the improved RSA. A new framework to dynamically adjust the trust region (TR) with respect to the sampling region (SR) is being investigated to exploit the more predictive RSA's.

Acknowledgments

This multidisciplinary research effort is supported in part by the following grants and contracts; NSF grants DMI94-57179 and DMI98-12857, NASA grant NAG1-2240 and CONACyT, Mexico.

References

1.- Alexandrov, N., 1996: Robustness Properties of a Trust Region Framework for Managing Approximations in Engineering Optimization, *Proceedings of the 6th AIAA/NASA/USAF Multidisciplinary Analysis & Optimization Symposium*, AIAA 96-4102, pp. 1056 - 1059, Bellevue, WA,September 4-6.

2.- Alexandrov, N. M.; Dennis, J. E.; Lewis, R. M.; Torczon, V., 1998: A Trust Region Framework for Managing Use

of Approximation Models in Optimization, *Structural Optimization*, Vol. 15, No. 1, pp. 16-23.

3.- Alexandrov, N. 1998: On Managing the Use of Surrogates in General Nonlinear Optimization and MDO. *Proceedings of the 7th AIAA/USAF/NASA/ISSMO Multidisciplinary Analysis & Optimization Symposium*, AIAA 98-4798, pp. 720 - 729, St. Louis, MO, September.

4.- Alexandrov, N. and Dennis, J.E., 1999: A Class of General Trust Region Multilevel Algorithms for Systems of Nonlinear Equations and Equality Constrained Optimization: Global Convergence Theory, *SIAM Journal on Optimization*, (in review).

5.- Balabanov, V., Kaufman, M., Knill, D.L., Haim, D., Golovidov, O., Giunta, A.A., Haftka, R.T., Grossman, B., Mason, W.H., Watson, L.T., 1996: Dependence of Optimal Structural Weight on Aerodynamic Shape for a High Speed Civil Transport. *Proceedings of the 6th AIAA/NASA/USAF Multidisciplinary Analysis & Optimization Symposium*, AIAA 96-4046, pp. 599 - 613, Bellevue, WA,September 4-6.

6.- Barthelemy, J. F.; Haftka, R. T. 1993: Approximation Concepts for Optimum Structural Design - A Review. *Structural Optimization*, 5, 129–144.

7.- Booker, A.J., Dennis, J.E., Frank, P.D., Sera£ni, D.B., Torcson, V., Trosset, M.W., 1999: A Rigorous Framework for Optimization of Expensive Functions by Surrogates, *Structural Optimization*, Vol. 17, No. 1, pp. 1-13.

8.- Box, G.; Hunter, W.; Hunter J. 1978: *Statistics for Experiments*. John Wiley and Sons.

9.- Chen, W., Tsui, K-L., Allen, J.K., Mistree, F., 1995: Integration of the Response Surface Methodology with the Compromise Decision Support Problem in Developing a General Robust Design Procedure, *Proceedings of the 1995 Design Engineering Technical Conferences, Advances in Design Automation*, ASME DE-Vol. 82, pp. 485 - 492, eds. S. Azarm, et al., Boston, Massachusetts, Sept. 17-21.

10.- Chen, W., Allen, J.K., Schrage, D.P., Mistree, F., 1996: Statistical Experimentation for Affordable Concurrent Design, *Proceedings of the 6th AIAA/NASA/USAF Multidisciplinary Analysis & Optimization Symposium*, AIAA 96-4085, pp. 921 - 930, Bellevue, WA, September 4-6.

11.- Chen, W., Simpson, T.W., Allen, J.K., Mistree, F., 1996: Using Design Capability Indices to Satisfy Sets of Design Requirements, *Proceedings of the 1996 ASME Design Engineering Technical Conference and Computers in Engineering Conference*, ASME Paper 96-DETC / DAC-1090, CD-ROM Proceedings, ISBN 0-7918-1232-4, Irvine, CA, August 18 -22.

12.- Gill, P. E.; Murray, W.; Wright, M.H.; 1989: *Numerical Linear Algebra and Optimization, Volume 1*, Addison Wesley.

13.- Giunta, A.A., Dudley, J.M., Narducci, R., Grossman, B., Haftka, R.T., Mason, W.H., Watson, L.T., 1994: Noisy Aerodynamic Response and Smooth Approximations in HSCT Design, *Proceedings of the Fifth AIAA/USAF/NASA/ISSMO Symposium*, AIAA 94-4376, pp. 1117 -1128, Panama City, Florida, September 7-9.

14.- Giunta, A.; Watson, L. 1998: A Comparison of Approximation Modeling Techniques: Polynomial Versus Interpolating Models. *Proceedings of the 7th AIAA/USAF/NASA/-ISSMO Multidisciplinary Analysis & Optimization Symposium*, AIAA 98-4758, pp. 392–404, St Louis, MO.

15.- Hedayat, A. S., Sloane, N.J.A., Stufken, J., 1999: *Orthogonal Arrays Theory and Applications*, Springer Series in Statistics, Springer-Verlag.

16.- Koch, P.N., Barlow, A., Allen, J.K., Mistree, F., 1996: Con£guring Turbine Propulsion Systems Using Robust Concept Exploration, *Proceedings of the 1996 ASME Design Engineering Technical Conference and Computers in Engineering Conference*, ASME Paper 96-DETC / DAC-1472, CD-ROM Proceedings, ISBN 0-7918-1232-4, Irvine, CA, August 18 -22.

17.- Lautenschlager, U., Eschenauer, H.A., Mistree, F., 1996: Components of Turbo Systems-A Proposal for Finding Better Layouts, *Proceedings of the 6th AIAA/NASA/USAF Multidisciplinary Analysis & Optimization Symposium*, AIAA 96-4096, pp. 1025 - 1035, Bellevue, WA, September 4-6.

18.- Lewis, R.M., 1996: A Trust Region Framework for Managing Approximation Models in Engineering Optimization. *Proceedings of the 6th AIAA/NASA/USAF Multidisciplinary Analysis & Optimization Symposium*, AIAA 96-4101, pp. 1053 - 1055, Bellevue, WA,September 4-6.

19.- Owen, A.B. (1992): Orthogonal Arrays for Computer Experiments, Integration and Visualization. *Statistica Sinica*, Vol. 2, No. 2, July, pp. 439–452

20.- Renaud, J. E. and Gabriele, G. A., 1993: Improved Coordination in Nonhierarchic System Optimization. *AIAA Journal*, Volume 31, Number 12, December, pp. 2367–2373.

21.- Renaud, J. E. and Gabriele, G. A.,1994: Approximation in Nonhierarchic System Optimization. *AIAA Journal*, Volume 32, Number 1, January, pp. 198–205.

22.- Rodríguez, J. F.; Renaud, J. E.; Watson, L. T. 1998: Convergence of Trust Region Augmented Lagrangian Methods Using Variable Fidelity Approximation Data. *Structural Optimization*, 15, pp. 141–156.

23.- Rodríguez, J. F.; Renaud, J. E.; Watson, L. T. 1998: Trust Region Augmented Lagrangian Methods for Sequential Response Surface Approximation and Optimization. *Journal of Mechanical Design*, Vol. 120, pp. 58–66.

24.- Rodríguez, J.F., Perez, V., Renaud, J.E., Padmanabhan, D., 2000: Sequential Approximate Optimization Using Variable Fidelity Response Surface Approximations. *Proceedings of the 41st AIAA/ASME/ASCE/ AHS/ASC Structures, Structural Dynamics, and Materials Conference*, AIAA 2000-1391, Atlanta, GA, April 3-6.

25.- Rodríguez, J. F., Renaud, J. E., Wujek, B. A., Tappeta, R. V., Trust Region Model Management in Multidisciplinary Design Optimization, *Journal of Computational and Applied Mathematics*. (accepted for publication)

26.- Roux, W.J., Stander, N., Haftka, R.T., 1996: Response

Surface Approximations for Structural Optimization, *Proceedings of the 6th AIAA/NASA/USAF Multidisciplinary Analysis & Optimization Symposium*, AIAA 96-4042, pp. 565 - 578, Bellevue, WA,September 4-6.

27.- Sellar, R.S., Batill, S.M. and Renaud, J.E., 1996: A Neural Network-Based, Concurrent Subspace Optimization Approach to Multidisciplinary Design Optimization. *34th AIAA Aerospace Sciences Meeting*, AIAA 96-0714, Reno, NV, January 15-18.

28.- Simpson, T.W., Chen, W., Allen, J.K., Mistree, F., 1996: Conceptual Design of a Family of Products Through the Use of the Robust Concept Exploration Method. *Proceedings of the 6th AIAA/NASA/USAF Multidisciplinary Analysis & Optimization Symposium*, AIAA 96-4161, pp. 1535 - 1545, Bellevue, WA, September 4-6.

29.- Sobieszczanski-Sobieski, J. 1988: Optimization by Decomposition: A Step from Hierarchic to Non-Hierarchic Systems. *Second NASA/Air Force Symposium on Recent Advances in Multidisciplinary Analysis and Optimization* (held at Hampton, VA). NASA Conference Publication 3031, Part 1. 28–30.

30.- Sobieszczanski-Sobieski, J. 1990: Sensitivity of Complex, Internally Coupled Systems. *AIAA Journal*. Vol. 28, No. 1, January, pp. 153-160.

31.- Sobieszczanski-Sobieski, J.; Bloebaum, C. L. ; Hajela, P.1990: Sensitivity of Control-Augmented Structure Obtained by a System Decomposition Method. *AIAA Journal*. Vol. 29, No. 2, February, pp. 264–270.

32.- Tappeta, R. V., Nagendra, S., Renaud, J.E, 1999: A Multidisciplinary Design Optimization Approach for High Temperature Aircraft Engine Components, *Structural Optimization*, Volume 18, Number 2/3, October, pp. 134-145, Published by Springer-Verlag, Germany.

33.- Torczon, V.; Trosset, M. W. 1998: Using Approximations to Accelerate Engineering Design Optimization. *Proceedings of the 7th AIAA/USAF/NASA/ISSMO Multidisciplinary Analysis & Optimization Symposium* (held at Saint Louis, Missouri), Paper 98-4800, pp. 507–512.

34.- Vanderplaats, G.N., 1999, *Numerical Optimization Techniques for Engineering Design*, Vanderplaats Research and Development Inc., Colorado Springs, CO.

35.- Venter, G., Haftka, R.T., Starnes, J.H., 1996: Construction of Response Surfaces for Design Optimization Applications. *Proceedings of the 6th AIAA/NASA/USAF Multidisciplinary Analysis & Optimization Symposium*, AIAA 96-4040, pp. 548 - 564, Bellevue, WA,September 4-6.

36.- Wujek,B., Renaud, J.E., Batill. S.M., Brockman, J.B., 1996: Concurrent Subspace Optimization Using Design Variable Sharing in a Distributed Computing Environment. *Concurrent Engineering: Research and Applications (CERA)*, December, Published by Technomic Publishing Company, Inc, USA.

37.- Wujek, B. A.; Renaud, J. E.; Batill, S. M. 1997: A Concurrent Engineering Approach for Multidisciplinary Design in a Distributed Computing Environment. In: N. Alexandrov and M.Y. Hussaini (eds), *Multidisciplinary Design Optimization: State-of-the-Art*, Proceedings in Applied Mathematics 80, pp. 189–208. Philadelphia: SIAM.

38.- Wujek, B. A. and Renaud, J. E., 1998: A New Adaptive Move-Limit Management Strategy for Approximate Optimization, Part I. *AIAA Journal*, Volume 36, Number 10, October, pp. 1911–1921.

39.- Wujek, B. A. and Renaud, J. E., 1998: A New Adaptive Move-Limit Management Strategy for Approximate Optimization, Part II. *AIAA Journal*, Volume 36, Number 10, October, pp. 1922–1937.

40.- Zoutendijk, G., 1960: *Methods of Feasible Directions*, Elsevier.